

**Origin of ferromagnetism in molybdenum dioxide from *ab initio* calculations**Jawad Nisar,<sup>1,\*†</sup> Xiangyang Peng,<sup>1,\*‡</sup> and Rajeev Ahuja<sup>1,2</sup><sup>1</sup>*Condensed Matter Theory Group, Department of Physics and Materials Science, Uppsala University, P.O. Box 530, S-751 21 Uppsala, Sweden*<sup>2</sup>*Applied Materials Physics, Department of Materials and Engineering, Royal Institute of Technology (KTH), S-100 44 Stockholm, Sweden*

(Received 1 September 2009; published 13 January 2010)

We have performed spin-polarized calculations of the unexpected ferromagnetism in ultrathin films of molybdenum dioxide ( $\text{MoO}_2$ ) within the framework of density-functional theory. It is found that the ideal bulk  $\text{MoO}_2$  is metallic and nonmagnetic. Bulk  $\text{MoO}_2$  with Mo vacancy, O vacancy, Mo interstitial, or O interstitial remains to be nonmagnetic. Using slab calculation, we observed ferromagnetism in both oxygen-rich and -poor  $\text{MoO}_2$  (100) surfaces with average surface magnetic moment 1.53 and  $0.69\mu_B$  per surface Mo atom, respectively. The partial density of states of surface Mo atom at the Fermi level ( $E_F$ ) is much larger than that of the Mo atom in the center of the slab and in bulk  $\text{MoO}_2$ , which indicates that ferromagnetism in surface (100) is due to Stoner instability. Enrichment of oxygen at the surface is found to be more favorable for ferromagnetism in  $\text{MoO}_2$  (100). The  $2p$  states of surface oxygen atoms are significantly hybridized with the  $4d$  states of Mo atoms and are appreciably spin polarized.

DOI: [10.1103/PhysRevB.81.012402](https://doi.org/10.1103/PhysRevB.81.012402)

PACS number(s): 75.70.Rf, 61.72.Bb

Spintronics materials have large potential in the field of data processing, data storage, transmission of digital information and magnetic sensor. These materials have the capacity to integrate the electronic and magnetic properties in a single material, which produce high speed, low cost, and small-sized devices operating at very low power. Diluted magnetic semiconductors (DMS), obtained by doping transition metals and sometimes even nontransition metals in semiconductors, are promising spintronic materials. However, the material issues related to DMS, such as uniform doping and secondary phase, are still hard to solve. Therefore, the undoped pure spintronics materials offer another approach, which is free of these problems, and they are under active investigation. Ferromagnetism at room temperature has been found in undoped  $\text{HfO}_2$ ,  $\text{TiO}_2$ ,  $\text{In}_2\text{O}_3$ ,  $\text{ZnO}$ , and  $\text{SnO}_2$  films.<sup>1-4</sup> Some metal oxides such as  $\text{CeO}_2$ ,  $\text{Al}_2\text{O}_3$ ,  $\text{ZnO}$ ,  $\text{In}_2\text{O}_3$ , and  $\text{SnO}_2$  are not magnetic in bulk but show ferromagnetism at room temperature in their nanoparticles<sup>5</sup> with diameter 7–30 nm. The origin of ferromagnetism in films and nanoparticles may be due to defects, such as vacancies and interstitials, size effect and low dimensionality. For example, it is found that the  $d^0$  magnetism observed in  $\text{HfO}_2$  can be driven by the intrinsic point defects of Hf.<sup>1</sup> Surface states and surface resonance states can also play an important role in the magnetism process; it may lead to magnetic behavior which has not been seen in bulk materials. Surface ferromagnetism of transition metals such as Cr (001), V (100), and Fe (001) has been studied by first-principles calculations.<sup>6-8</sup>

Molybdenum-based materials are used to form the stable coordination environments and have been widely used as catalyst in the petrochemical industry for selective oxidation and isomerization of hydrocarbons.<sup>9</sup>  $\text{MoO}_2$  is a suitable commercial anode material for rechargeable lithium-ion batteries.<sup>10,11</sup> It also has exceptional optoelectronic properties, which have wide applications. However, its magnetic properties have not been much explored, since bulk  $\text{MoO}_2$  is a nonmagnetic material.<sup>12,13</sup> Although doping Fe atoms in

$\text{MoO}_2$  (100) films can lead to room-temperature ferromagnetism, the problem of precipitation of dopants still remains. Surprisingly, it is observed recently that the highly  $a$  axis oriented *undoped* thin film of  $\text{MoO}_2$  shows ferromagnetism at room temperature by near-edge x-ray absorption fine structure and x-ray magnetic circular dichroism experiments.<sup>14</sup> The ferromagnetism of clean  $\text{MoO}_2$  is very desirable not only because there is no issue of precipitation but also there is no compromise of other good properties of  $\text{MoO}_2$  due to introducing of alien atoms. The ferromagnetism of the clean  $\text{MoO}_2$  film, in combination with the existing exceptional properties of  $\text{MoO}_2$ , will bring novel and important applications. The unexpected ferromagnetism requires a new understanding and calls for explanations. In this Brief Report, we have performed detailed computational study of  $\text{MoO}_2$ , with a goal of identifying the origin of the ferromagnetism of undoped  $\text{MoO}_2$  film. Unlike  $\text{HfO}_2$ , it is found that defects, such as Mo and O vacancies and Mo and O interstitials cannot induce magnetism in  $\text{MoO}_2$ . Instead, the surface effect is found to significantly enhance the density of states (DOS) of the surface Mo atoms at the Fermi level, and hence induce the magnetic instabilities. In oxygen-rich surfaces, the larger magnetization and more stable ferromagnetism are observed.

The first-principles calculations were performed using projected augmented wave method<sup>15</sup> as implemented in Vienna *ab initio* simulation package.<sup>16,17</sup> The Perdew-Burke-Ernzerhof generalized gradient approximation (GGA-PBE)<sup>18,19</sup> was used for the exchange-correlation potential. The test of energy cutoff from 300 to 600 eV shows that 350 eV is already accurate enough. The plane-wave cutoff energy in our calculations is set to 400 eV. The atomic geometries are fully optimized until the forces on each atom are less than the threshold value of  $10^{-4}$  eV/Å. The molybdenum potential with  $4p$ ,  $5s$ , and  $4d$  electrons as valence states and the oxygen potential with  $2s$  and  $2p$  electrons as valence states have been used. The Gaussian smearing width is 0.2 eV. All Brillouin zone integrations are performed with

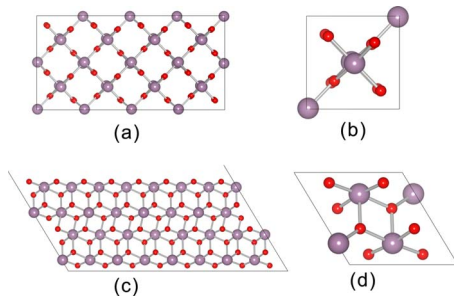


FIG. 1. (Color online) (a) and (b) are the view along (100) direction, (c) and (d) are the side view of surface and bulk MoO<sub>2</sub>. The small red spheres are oxygen and the large spheres are molybdenum.

a Monkhorst-Pack generated  $k$ -points mesh.<sup>20</sup>  $k$ -points mesh  $2 \times 2 \times 2$  and  $1 \times 2 \times 1$  were found to be sufficient to reach convergence for bulk and surface calculations, respectively. MoO<sub>2</sub> is the monoclinic structure with space group  $P2_1/c$  at ambient conditions. The calculated lattice parameters are  $a=5.76$  Å,  $b=4.901$  Å,  $c=5.687$  Å, and  $\beta=121.5^\circ$  within GGA, in good agreement with experimental data ( $a=5.6109$  Å,  $b=4.8562$  Å,  $c=5.6285$  Å, and  $\beta=120.95^\circ$ ).<sup>21</sup> The original unit cell is expanded to a  $(2 \times 2 \times 2)$  supercell containing 96 atoms in total for bulk calculations. The MoO<sub>2</sub> (100) surface is simulated by slab model. The four-layer slab of MoO<sub>2</sub> is chosen for calculation of the surface. The size of the slab is  $2 \times 2 \times 4$  with 192 atoms in the whole slab model. The number of layers in slab is very important for periodic slab model to get reasonable results. For this purpose, we have performed several tests to assess the convergence of the surface energy with respect to the number of layers (up to six) using PBE. All atomic positions were relaxed during these calculations. Surface energies were calculated as

$$E_{surf} = \frac{E_{slab} - E_{MoO_2} N_{MoO_2}}{2S},$$

where  $E_{slab}$  is the total energy of the supercell,  $E_{MoO_2}$  is the reference energy for a MoO<sub>2</sub> unit in the bulk phase,  $N_{MoO_2}$  is the number of MoO<sub>2</sub> unit in the supercell, and  $S$  the surface area of one side of the slab. It is observed that surface energy is quite similar for the slabs of four and six layers, which is found to be around 1.77 J/m<sup>2</sup>. Therefore, the four-layer slab of MoO<sub>2</sub> is chosen for all calculations. We tried different vacuum sizes and found that a vacuum of thickness of 12 Å is enough to decouple the adjacent slabs. Figure 1 shows the optimized atomic structure of the ferromagnetic (FM) MoO<sub>2</sub> (100) surface and bulk MoO<sub>2</sub>. Ferromagnetic stability is assessed by calculating the total energy difference between the antiferromagnetic (antiparallel) configuration and ferromagnetic (parallel) configuration. The system is ferromagnetic if the ferromagnetic configuration has the lower total energy.

First we have studied the magnetic properties of ideal bulk MoO<sub>2</sub>, which is found to be a nonmagnetic metal. Defects in bulk materials can play an important role with respect to electronic and magnetic properties of the system. Bulk HfO<sub>2</sub> is also found to be nonmagnetic if it is defectless.

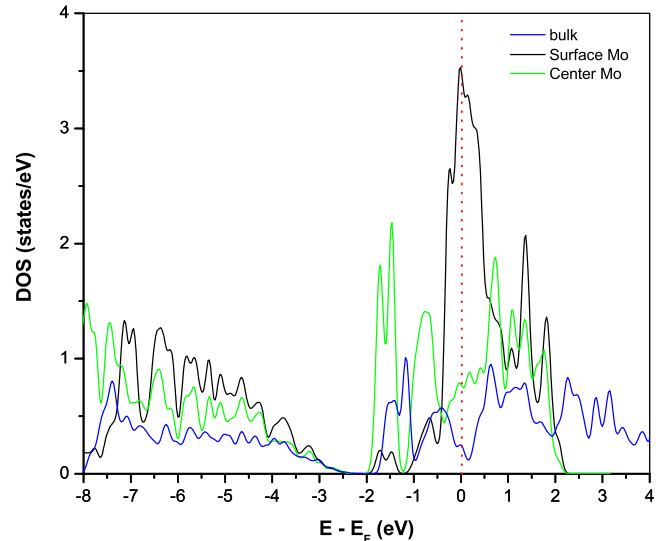


FIG. 2. (Color online) DOS of bulk, surface, and center molybdenum atom for molybdenum dioxide (100) surface (nonspin-polarized calculation), the vertical red dot line indicate Fermi level ( $E_F=0$  eV).

After introducing Hf vacancies, it becomes ferromagnetic.<sup>1</sup>

We have also studied bulk MoO<sub>2</sub> with Mo or O vacancies and found that vacancies cannot induce magnetism in MoO<sub>2</sub>. The different role of vacancies played in bulk MoO<sub>2</sub> and bulk HfO<sub>2</sub> is maybe due to their different electronic structures. In bulk HfO<sub>2</sub>, all of Hf valence electrons are transferred to O and form ionic bonds, giving rise to large energy gap. After introducing Hf vacancy, the electrons in the O atoms near the Hf vacancy are quite localized and occupy the gap states. Therefore, the magnetic moments are mainly localized in the O atoms close to Hf vacancy. The electronic configuration of Mo atom is  $4d^5 5s^1$ . In MoO<sub>2</sub>, Mo has a valence of +4 and has two  $4d$  electrons unbound. In the DOS of ideal bulk MoO<sub>2</sub>, one can see that the states at the Fermi level are mainly from the  $d$  states of the unbound  $d$  electrons of Mo (Fig. 2). Therefore, the unbound  $d$  electrons in Mo atoms are itinerant electrons. Therefore the mechanism of the ferromagnetism observed experimentally in MoO<sub>2</sub> and HfO<sub>2</sub> should be different. Further considering Mo and O interstitials in bulk MoO<sub>2</sub>, our calculations still show that MoO<sub>2</sub> is not magnetic. Thus, it is not likely that the experimentally observed ferromagnetism in MoO<sub>2</sub> films is due to the defects.

Apart from defects, reducing the dimensionality of the material can also affect the electric and magnetic properties. It has been found that some materials, which are otherwise nonmagnetic, possess surface ferromagnetism.<sup>6-8</sup> We studied a axis oriented *undoped* thin film of MoO<sub>2</sub> by using slab model. It is observed from calculations that oxygen terminated or oxygen enriched the MoO<sub>2</sub> (100) surface is ferromagnetic. The ferromagnetic configuration is lower in energy than the antiferromagnetic (AFM) configuration by 351 meV. The magnetic moments are mainly localized at the first surface Mo layer. Each Mo atom in the first surface layer has magnetic moment of about  $1.53\mu_B$ . The magnetic moment of the second Mo surface layer is abruptly reduced with a mag-

netic moment  $0.11\mu_B$  per Mo atom. The magnetic moments come from the  $4d$  orbital of Mo in the first layer. In contrast, the magnetic moments in  $\text{HfO}_2$  are mainly due to the  $2p$  gap states of the oxygen atoms close to the Hf vacancy.<sup>1</sup>

We have also studied the oxygen-deficient surface by removing the outmost oxygen layer in the formerly studied oxygen-rich slab. Interestingly, it is observed that after relaxation of the system, oxygen atoms initially below the first Mo layer move outwards to the surface and finally occupy topmost positions. This indicates that no matter the  $\text{MoO}_2$  (100) surface is O rich or deficient, it tends to be oxygen terminated. The oxygen-deficient  $\text{MoO}_2$  (100) surface is also found to be ferromagnetic. The average magnetic moment  $0.69\mu_B$  per surface Mo atom is smaller than that in oxygen-rich (100) surface. The energy of ferromagnetic order is 286.8 meV lower than that of antiferromagnetic order per unit cell, showing that the FM order is more stable in oxygen-rich surface than in oxygen-deficient surface. Since both oxygen rich and deficient surfaces are ferromagnetic,  $\text{MoO}_2$  (100) is a robustly ferromagnetic surface.

The origin of the surface ferromagnetism of  $\text{MoO}_2$  (100) can be understood within the framework of Stoner's theory. We have calculated the nonspin-polarized partial DOS (PDOS) of Mo in the first surface layer and the second layer of  $\text{MoO}_2$  slab, and the PDOS of Mo atom in bulk  $\text{MoO}_2$ , as shown in Fig. 2. It can be observed that the PDOS of the first surface Mo at Fermi level is much larger than that of Mo in the bulk. The reduced coordination number and the lower symmetry at the surface gives rise to the significant enhancement of the PDOS of surface Mo at Fermi level ( $E_F$ ), resulting in "Stoner" instability and inducing surface magnetism. Therefore, large band splitting in the vicinity of Fermi level due to ferromagnetic exchange interactions occur in the ferromagnetic  $\text{MoO}_2$  (100) surface. The PDOS of the second Mo layer at Fermi level is quickly reduced by three times. As a result, the second Mo layer is weakly magnetized with magnetic moment  $0.11\mu_B$  per Mo atom. The  $2p$  orbital of oxygen atom are hybridized with the  $4d$  orbital of Mo atoms. The PDOS of the O atom bonded to the first layer Mo atom overlaps with that of the latter at the Fermi level. Although, only weak magnetism with magnetic moment of  $0.02\mu_B$  per O atom is found in the surface oxygen atoms in  $\text{MoO}_2$  (100) film, the states of surface oxygen atoms are noticeably spin polarized, as shown in Fig. 3. This explains the magnetic polarization of the  $2p$  orbital of oxygen observed in the experiments.<sup>14</sup>

The charge density of the states 1 eV below the Fermi level is plotted in Fig. 4(a). It can be seen that the isosurface of the density of the electrons near the Fermi level, which give rise to magnetism, is connected and continuous in the whole space, indicating the itinerant character of these electrons. Spin charge density of  $\text{MoO}_2$  (100) film, as depicted in Fig. 4(b), show that the spin-polarized electrons are much localized in the first surface layer of Mo.

In the case of oxygen-deficient  $\text{MoO}_2$  (100), the PDOS of surface Mo atom also shows high peak at Fermi level as compared to the sublayer Mo atom. Stoner instability also occurs and leads to the ferromagnetism in oxygen-deficient (100) surface. The PDOS of surface Mo in oxygen-rich surface atom at Fermi level is larger than that in oxygen-

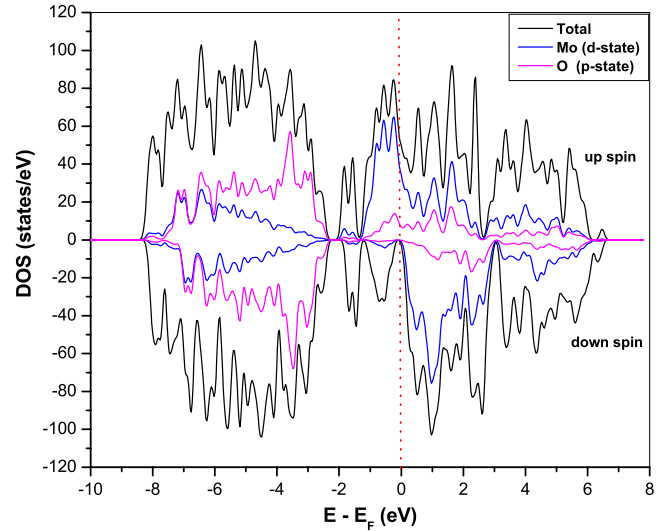


FIG. 3. (Color online) Total and partial DOS of Molybdenum dioxide (100) surface (spin-polarized calculation), the vertical red dot line indicate Fermi level ( $E_F=0$  eV).

deficient surface, indicating that the enrichment of oxygen at surface can facilitate the occurrence of ferromagnetism. This is also in agreement with the fact that the FM order is more favorable with respect to the AFM order as shown in Table I.

In summary, the ferromagnetism of undoped  $\text{MoO}_2$  has been investigated by *ab initio* calculations. These calculations show that ideal bulk  $\text{MoO}_2$  is a nonmagnetic metal and

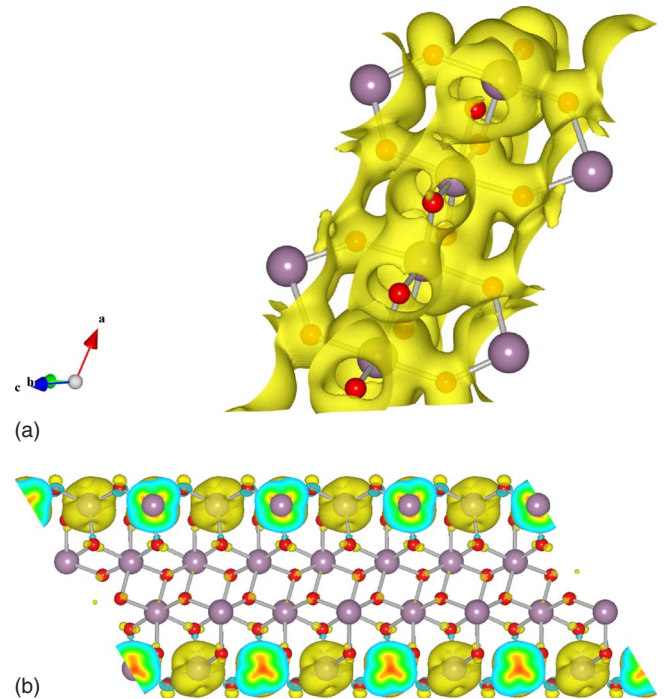


FIG. 4. (Color online) (a) The isosurface plot of the charge density of the states 1 eV below the Fermi level. The small red spheres are oxygen and the large spheres are molybdenum. For clarity, only part of the slab is shown. (b) Side view of the isosurface plot of spin charge density of the  $\text{MoO}_2$  (100) surface.

TABLE I. Total energy difference,  $\Delta E = E_{\text{AFM}} - E_{\text{FM}}$  between antiferromagnetic and ferromagnetic alignment of the magnetic moment and magnetic moment per Mo atom for different configurations of MoO<sub>2</sub>.

Surface	$\Delta E = E_{\text{AFM}} - E_{\text{FM}}$ (meV)	Magnetic moment/surface Mo atom ( $\mu_B$ )	Stability
(100)	351.0	1.53	FM
Mo-terminated (100)	286.8	0.69	FM

the states at Fermi level are mainly of *d* character. The defects, such as Mo and O vacancies or interstitials cannot induce spin polarization in MoO<sub>2</sub>. It is found that in the oxygen-rich or -deficient surface of MoO<sub>2</sub> (100), the surface ferromagnetism is stabilized, in good agreement with the experiments.<sup>14</sup> Although the magnetic moments are mainly localized in the first Mo layer, the states of oxygen atoms near the surface are noticeably spin polarized. The high peak of surface Mo atom at Fermi level ( $E_F$ ) indicates that the stoner instability is responsible for the ferromagnetism ob-

served in MoO<sub>2</sub> (100). Enrichment of oxygen at surface is expected to enhance the surface ferromagnetism possibly due to the increased *2p-4d* hybridization of surface Mo and O atoms.

We would like to acknowledge STINT and VR for financial support. One of us, J.N., also acknowledges Higher Education Commission (HEC) of Pakistan for financial support. SNIC and UPPMAX are acknowledged for providing computing time.

\*Corresponding author.

<sup>†</sup>jawad.nisar@fysik.uu.se

<sup>‡</sup>xiangyang.peng@fysik.uu.se

<sup>1</sup>C. D. Pemmaraju and S. Sanvito, Phys. Rev. Lett. **94**, 217205 (2005).

<sup>2</sup>N. H. Hong, J. Sakai, N. Poirot, and V. Brize, Phys. Rev. B **73**, 132404 (2006).

<sup>3</sup>Q. Y. Xu, H. Schmidt, S. Q. Zhou, K. Potzger, M. Helm, H. Hochmuth, M. Lorenz, A. Setzer, P. Esquinazi, C. Meinecke, and M. Grundmann, Appl. Phys. Lett. **92**, 082508 (2008).

<sup>4</sup>N. H. Hong, N. Poirot, and J. Sakai, Phys. Rev. B **77**, 033205 (2008).

<sup>5</sup>A. Sundaresan, R. Bhargavi, N. Rangarajan, U. Siddesh, and C. N. R. Rao, Phys. Rev. B **74**, 161306 (2006).

<sup>6</sup>C. L. Fu and A. J. Freeman, Phys. Rev. B **33**, 1755 (1986).

<sup>7</sup>S. Ohnishi, C. L. Fu, and A. J. Freeman, J. Magn. Magn. Mater. **50**, 161 (1985).

<sup>8</sup>S. Ohnishi, A. J. Freeman, and M. Weinert, Phys. Rev. B **28**, 6741 (1983).

<sup>9</sup>Y. Okamoto, N. Oshima, Y. Kobayashi, O. Terasaki, T. Kodaira, and T. Kubota, Phys. Chem. Chem. Phys. **4**, 2852 (2002).

<sup>10</sup>L. C. Yang, Q. S. Gao, Y. Tang, Y. P. Wu, and R. Holze, J. Power Sources **179**, 357 (2008).

<sup>11</sup>Y. Liang, S. Yang, Z. Yi, X. Lei, J. Sun, and Y. Zhou, Mater. Sci. Eng., B **121**, 152 (2005).

<sup>12</sup>M. A. Khillia, H. Mikhail, A. Aau-el Saud, and Z. M. Hanaf, Czech. J. Phys. B **30**, 1039 (1980).

<sup>13</sup>V. Eyert, R. Horny, K. H. Hock, and S. Horn, J. Phys.: Condens. Matter **12**, 4923 (2000).

<sup>14</sup>P. Thakur, J. C. Cezar, N. B. Brookes, R. J. Choudhary, Ram Prakash, D. M. Phase, K. H. Chae, and Ravi Kumar, Appl. Phys. Lett. **94**, 062501 (2009).

<sup>15</sup>P. E. Blochl, Phys. Rev. B **50**, 17953 (1994).

<sup>16</sup>G. Kresse and J. Hafner, Phys. Rev. B **49**, 14251 (1994).

<sup>17</sup>G. Kresse and D. Joubert, Phys. Rev. B **59**, 1758 (1999).

<sup>18</sup>J. P. Perdew, J. A. Chevary, S. H. Vosko, K. A. Jackson, M. R. Pederson, D. J. Singh, and C. Fiolhais, Phys. Rev. B **46**, 6671 (1992).

<sup>19</sup>J. P. Perdew and Y. Wang, Phys. Rev. B **45**, 13244 (1992).

<sup>20</sup>H. J. Monkhorst and J. D. Pack, Phys. Rev. B **13**, 5188 (1976).

<sup>21</sup>B. G. Brandt and A. C. Skapski, Acta Chem. Scand. **21**, 661 (1967).